The Journal of Immunology

CD4$^-$ Plasmacytoid Dendritic Cells (pDCs) Migrate in Lymph Nodes by CpG Inoculation and Represent a Potent Functional Subset of pDCs

Guo-Xiang Yang, Zhe-Xiong Lian, Kentaro Kikuchi, Yong-Jun Liu, Aftab A. Ansari, Susumu Ikehara and M. Eric Gershwin

J Immunol 2005; 174:3197-3203; ;
doi: 10.4049/jimmunol.174.6.3197
http://www.jimmunol.org/content/174/6/3197

The Journal of Immunology is published twice each month by
The American Association of Immunologists, Inc.,
1451 Rockville Pike, Suite 650, Rockville, MD 20852

Print ISSN: 0022-1767 Online ISSN: 1550-6606.

CD4$^-$ Plasmacytoid Dendritic Cells (pDCs) Migrate in Lymph Nodes by CpG Inoculation and Represent a Potent Functional Subset of pDCs

Guo-Xiang Yang,[1]* Zhe-Xiong Lian,[1]* Kentaro Kikuchi,* Yong-Jun Liu,[†] Aftab A. Ansari,[‡] Susumu Ikehara,[§] and M. Eric Gershwin[2]*

We have recently identified two groups of plasmacytoid dendritic cells (pDCs) isolated from murine liver based on the expression of CD4 and other cell surface markers uniquely expressed by pDCs. Herein, we describe the identification of both CD4$^+$ and CD4$^-$ pDCs that clearly exist in lymph nodes (LNs), spleen, liver, thymus, bone marrow, and lung. Normally, CD4$^+$ pDCs are enriched in LNs. However, after in vivo systemic injection with bacterial CpG, a larger number of CD4$^-$ pDCs are recruited to the LNs and local inoculation by CpG drives CD4$^-$ pDCs migrating into local sentinel LNs, suggesting that CD4$^-$ pDCs are the main subpopulation migrating to the peripheral LNs. Furthermore, although both freshly isolated CD4$^+$ pDCs and CD4$^-$ pDCs appear as an immature plasmacytoid cell and develop into a DC morphology following activation, the two subsets have strikingly different immune features, including differences in the production pattern of cytokines stimulated with CpG and in T cell activation. ***The Journal of Immunology,*** **2005, 174: 3197–3203.**

Dendritic cells (DCs)[3] are potent APCs documented to play a fundamental role in the initiation of the immune response (1, 2) and are strategically located in peripheral tissues where they can optimally survey for incoming pathogens. The interaction of DCs with pathogens leads to migration to secondary lymphoid organs where they initiate a specific immune response. Most DCs gain access from the afferent lymphatic vessels that drain peripheral tissues. However, plasmacytoid DCs (pDCs) appear to enter lymph nodes (LNs) via high endothelial venules (HEVs) directly from the blood and produce large amounts of type I IFN upon activation by a number of viruses (3). Compared with myeloid DC, human pDCs have a different migration pattern and synthesize chemokines. Although they fail to migrate in response to inflammatory chemokines, pDC are known to respond to LN-homing chemokines in vitro following CD40 ligation (4). Clearly, ethical issues prevent the studies of DC trafficking in humans but in mice, in vivo injection of CpG promotes the migration of Langerhans cells out of the epidermis and into LNs (5, 6). Similarly HSV-1 induced inflammation facilitates recruitment of murine pDC into sentinel LNs (7, 8). However, the pattern of migration of pDCs in vivo in response to infection remains unclear.

The identification of a murine counterpart of human pDCs provides a powerful laboratory tool for detailed investigation of the function and mechanism of this cell lineage. Murine pDCs have been isolated from nearly all lymphoid tissues, including spleen, LNs, thymus, bone marrow (BM), and even liver (9–16). Very recently, pDCs have been found in murine blood, which very closely resemble human pDCs found in peripheral blood (17). However, the pDCs are also heterogeneous in surface phenotype and function (14). Although it has been suggested that CD4$^-$ pDCs are the immediate precursors of CD4$^+$ pDCs, the in vivo functional implications of the pDC subsets remain to be determined.

We report herein that CD4$^-$ pDCs are more effective in the synthesis of IFN-α and in T cell activation. Further, CD4$^-$ pDCs develop into CD4$^+$ pDCs in recipient mice following adoptive transfer. These two subsets of murine pDCs represent distinct developmental stages of this cell lineage (14). We conclude that CD4$^-$ pDCs are the major source of pDCs that migrate into LNs in response to infection and produce IFN-α to trigger innate and adaptive immune reactions.

Materials and Methods

Animals

C57BL/6J (B6, Ly5.2) mice, congenic C57BL/6-Ly5.1-Pep3b (B6, Ly5.1) mice and BALB/c mice were obtained from The Jackson Laboratory. All mice were kept under specific pathogen-free conditions and used at 8–12 wk of age.

Antibodies

PE-conjugated CD11c (HL3), CD4 (GK1.5), CD19 (6D5), Flt3 (A2F10.1); biotin-conjugated CD8α (53-6.7), CD11c (HL3), CD19 (6D5), CD40 (3/23), CD80 (B7.1, 16-10A1), CD86 (B7.2, GL1), CD123 (IL-3R, 5B11), CD127 (IL-7R, A7R34), Sca-1 (E13-161.7), c-*kit* (CD117, 2B8), Ly-6C (AL-21), Gr-1 (Ly-6G, RB6-8C5), CD11b (Mac-1, M1/70), and TER119 (TER119) Abs were purchased from BD Pharmingen. FITC-conjugated CD4 (GK1.5), CD11c (HL3); biotin-conjugated NK1.1 (PK136), MHC class II (M5/114.15.2); PE-Cy5.5-conjugated Ly5.1 (CD45.1, A20), Ly5.2 (CD45.2, 104); purified CD3 (17A2), CD19 (6D5), CD11b (Mac-1, M1/70), Gr-1 (Ly6-G, RB6-8C5), CD122 (5H4), TER119 (TER119,) and CD16/32 (FcγIII/IIR, 93) Abs were purchased from e-Bioscience. Allophycocyanin-conjugated B220 (CD45R, RA3-6B2), biotin-conjugated TCR$\alpha\beta$ (H57-597) and PE-Cy5.5 or Tri-color conjugated streptavidin were

*Division of Rheumatology, Allergy and Clinical Immunology, University of California, Davis, CA 95616; [†]Department of Immunology, M. D. Anderson Cancer Center, Houston, TX 77030; [‡]Department of Pathology, Emory University School of Medicine, Atlanta, GA 30322; and [§]First Department of Pathology, Kansai Medical University, Osaka, Japan

Received for publication September 14, 2004. Accepted for publication December 20, 2004.

The costs of publication of this article were defrayed in part by the payment of page charges. This article must therefore be hereby marked *advertisement* in accordance with 18 U.S.C. Section 1734 solely to indicate this fact.

[1] G.-X.Y and Z.-X.L contributed equally to this work.

[2] Address correspondence and reprint requests to Dr. M. Eric Gershwin, Division of Rheumatology, Allergy and Clinical Immunology, University of California, One Shields Avenue, Davis, CA 95616. E-mail address: megershwin@ucdavis.edu

[3] Abbreviations used in this paper: DC, dendritic cell; LN, lymph node; BM, bone marrow; HEV, high endothelial venule; pDC, plasmacytoid DC; LD, low density; ODN, oligodeoxynucleotide; MLR, mixed lymphoid reaction; IPC, IFN-α-producing cell; SLE, systemic lupus erythematosus.

0022-1767/05/$02.00

purchased from Caltag Laboratories. All isotype controls were obtained from BD Pharmingen.

Isolation of pDC subsets

Spleen cells and LN cells were collected from 8- to 12-wk-old B6 Ly5.1 mice and filtered through a 100-μm mesh. After centrifugation, cells were resuspended with washing buffer consisting of PBS containing 0.2% BSA and overlaid on 1.071 Optiprep (Nycomed Pharma) solution diluted with PBS (containing 0.2% BSA). The gradient was centrifuged at 750 $\times$ *g* for 20 min at 20°C. The low density (LD) cells at the washing buffer/Optiprep solution interface were collected, resuspended in washing buffer, and recovered by centrifugation. For pDC sorting, the LD cells were incubated with a mixture of mAbs against CD3, CD19, Mac-1, Gr-1, TER119, followed by the addition of sheep anti-rat IgG-conjugated magnetic-beads (Dynabeads; Dynal Biotech) to deplete the Ab-bound cells. The leftover DC-enriched cells were stained with anti-CD4-FITC, anti-B220-allophycocyanin, anti-CD11c-PE, and anti-NK1.1, TCR$\alpha\beta$-biotin, followed by Tri-color-conjugated streptavidin staining. After washing, cells were sorted into the following fractions: NK1.1$^-$TCR$\alpha\beta^-$CD11c$^+$B220$^+$CD4$^+$ (CD4$^+$ pDCs), NK1.1$^-$TCR$\alpha\beta^-$CD11c$^+$B220$^+$CD4$^-$ (CD4$^-$ pDCs) populations by a 10-parameter MoFlo cell sorter (Cytomation). The purity of sorted cells was determined by reanalyzing a small sample of the collected cells and was >97%.

For cell surface staining, the LD cells were stained with a mixture of mAbs against CD3, CD19, Mac-1, Gr-1, and TER119. To remove the contaminating NK cell, purified rat-anti-mouse-CD122 was also added. Sheep anti-rat IgG-conjugated magnetic-beads (Dynabeads) were used to deplete the Ab-bound cells. The DC-enriched cells were stained with anti-CD4-FITC, anti-B220-allophycocyanin, anti-CD11c-PE, and different Abs labeled by biotin, followed by PE-Cy5.5-conjugated streptavidin staining. Before staining, FcγII/III receptors on the cells were blocked by preincubation of the samples with a Fc Block (CD16/32) to reduce nonspecific staining (except for the evaluation of CD16/32 expression). After washing with washing buffer, the cells were acquired and analyzed on a dual-laser FACSCalibur (BD Biosciences) using CellQuest software (BD Biosciences).

Transplantation of pDCs

Female B6 Ly5.1-recipient mice were irradiated with 5 Gy 7–8 h before transplantation. A total of 5–7 $\times$ 10^5 CD4$^+$ or CD4$^-$ pDCs sorted from B6 Ly5.2 mice were injected intrasplenically into the recipient (18). Animals were maintained in a pathogen-free environment and aqueous antibiotics were added to the drinking water. Three days after transplantation, recipient mice were sacrificed and spleen cells analyzed on a dual-laser FACSCalibur using CellQuest software (BD Biosciences).

Some mice were transplanted with CFSE-labeled CD4$^+$ or CD4$^-$ pDCs to observe cell division. For CFSE labeling, purified CD4$^+$ and CD4$^-$ pDCs were incubated with 10 μM CFSE (Molecular Probes) for 10 min at 37°C and washed once with PBS. These cells were incubated in prewarmed RPMI 1640 for another 30 min to ensure complete modification of the probe and washed again. CFSE-labeled cells were injected intrasplenically into the recipient mice.

In vivo CpG inoculation

For systemic injection of CpG, 100 μl of 100 μM CpG-B (oligodeoxynucleotide (ODN) 2006: tcg tcg ttt tgt cgt ttt gtc gtt (19), purchased from TriLink BioTechnologies) suspended in PBS were i.v. injected in the mice via tail vein (~65 μg/mouse). Control mice were injected with the same volume of PBS. After 1 day, the infected mice were killed and pDCs were analyzed in LN, spleen, thymus, liver, and BM by flow cytometry. For local injection of CpG, 50 μl of 100 μM CpG-B were injected s.c. in the left hind legs of mice. As a control, PBS was injected in the right hind legs. After 1 day, bilateral inguinal nodes were excised. pDCs were analyzed by flow cytometry.

RT-PCR

Total RNA was extracted from sorted CD4$^+$ and CD4$^-$ pDCs subsets using the RNeasy kit (Qiagen). After DNase I treatment, first-strand cDNA was synthesized using Superscript II (Invitrogen Life Technologies) and random hexamer primer (Invitrogen Life Technologies) in the presence of an RNase inhibitor. PCR was performed in a GeneAmp PCR System 9700 (Applied Biosystems) with Ampli*Taq* Gold enzyme and buffer (PerkinElmer). For real-time quantitative RT-PCR, the cDNA of each population was analyzed for the expression of the CCR7 gene using SYBR Green Supermix with Rox (Bio-Rad) and the 7900HT Sequence Detection system (Applied Biosystems). The primers used are shown in Table I.

Measurement of cytokine production

All cell cultures were performed in RPMI 1640 culture medium (Invitrogen Life Technologies) supplemented with 10% FCS, 100 μg/ml streptomycin, and 100 U/ml penicillin (Invitrogen Life Technologies). Aliquots of 3 $\times$ 10^4 sorted CD4$^+$ or CD4$^-$ pDCs were cultured in 200 μl of RPMI 1640 medium in round-bottom 96-well plates at 37°C in the absence or presence of the CpG-A (2 μM) (ODN 2216: ggG GGA CGA TCG TCg ggg gG (19), purchased from Invivogen) or CpG-B (2 μM). Lowercase letters dictate phosphorothioate linkage. After 48 h in culture, supernatants were collected and analyzed using ELISA kits for the following cytokines: IFN-α (PBL Biomedical Laboratories), IL-6, IL-12 (p40), and TNF-α (R&D Systems), with known standards.

Mixed lymphoid reaction (MLR)

Spleen cells collected from BALB/c (H-2K^d) mice were overlaid onto Histopaque-1.077 (Sigma-Aldrich) and centrifuged for 20 min at 750 $\times$ *g*. LD cells were collected from the interface and after washing with PBS, incubated with a mixture of mAbs consisting of anti-CD8, anti-Mac-1/Gr-1, anti-CD11c, anti-CD19, anti-B220 and anti-TER119. Cells binding the mAbs were depleted using anti-rat Ig magnetic beads (Dynabeads). The CD4$^+$ T cells were then purified in the remaining cells by positive selection with CD4$^+$ microbeads and MiniMacs separation columns (Miltenyi Biotec).

For MLR assay, 15 $\times$ 10^4 CFSE labeling or unlabeling CD4$^+$ T cells were cocultured in triplicate with freshly isolated CD4$^+$ or CD4$^-$ pDCs (3 $\times$ 10^4) in the presence or absence of CpG-B (2 μM) in 200 μl of RPMI 1640 culture medium for 5 days in round-bottom 96-well plates. Proliferation of CFSE-labeled cells was measured as a loss of CFSE concentration determined by flow cytometry. In the culture group of CFSE-unlabeled CD4$^+$ cells, [^{3}H]thymidine (1 μCi/well) was added during the last 18 h of culture and the uptake of [^{3}H]TdR measured in a liquid scintillation counter (PerkinElmer Life Sciences). The mean cpm of triplicate cultures was calculated.

Statistical analyses

Differences in the proportion and number of increased cells, the amount of cytokine production among pDCs subsets, and the degree of T cell proliferation were analyzed using the unpaired Student *t* test (Statview); $p < 0.05$ was considered to be statistically significant.

Results

Distributions, characteristics, and relationship of pDC subsets

pDCs have been found to exist in both lymphoid and nonlymphoid organs (9–16). According to CD4 expression, CD11c$^+$B220$^+$ pDCs can be clearly subdivided into CD4$^+$ and CD4$^-$ pDC subsets in the spleen, LNs, BM, liver, thymus, and even lung of normal adult mice (Fig. 1). Moreover, the two pDC subsets were also detected in these organs of 12-mo-old B6 mice and their percentages did not reveal significant differences (data not shown). These results indicate that the CD4$^+$ and CD4$^-$ pDCs are neither organ- nor age-restricted. To characterize differences in the expression of cell surface molecules between the two pDC subsets, we isolated spleen CD4$^+$ and CD4$^-$ pDCs (Fig. 2*A*) and analyzed their phenotypes by four-color flow cytometry. Both CD4$^+$ and CD4$^-$ are

Table I. *PCR primer sequences*

	Forward Primer	Reverse Primer
CCR5	ACT TGG GTG GTG GCT GTG TTT	TTG TCT TGC TGG AAA ATT GAA
CCR6	CTG CAG TTC GAA GTC ATC	GTC ATC ACC ACC ATA ATG TTG
CCR7	AGC ACC ATG GAC CCA GGG AAA CC	CAG CAT CCA GAT GCC CAC A

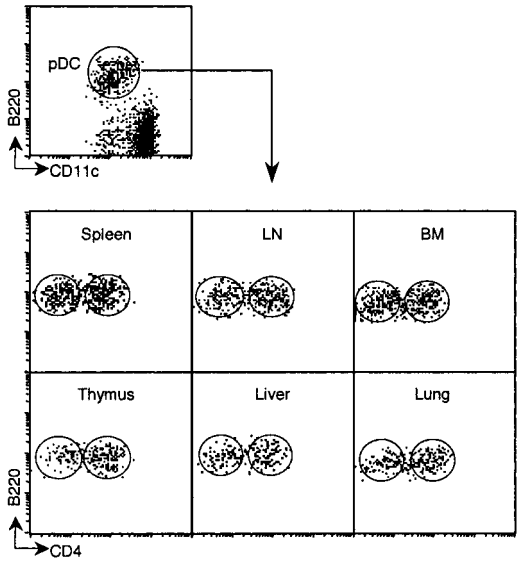

FIGURE 1. Distribution of pDC subsets. Freshly isolated spleen, LNs, BM, liver, thymus, and lung LD cells (1.071) were stained with CD4-FITC, CD11c-PE, B220-allophycocyanin, and NK1.1-biotin, followed by staining with PE-Cy5.5-conjugated streptavidin. Stained cells were analyzed by four-color flow cytometry. The NK1.1$^-$CD11c$^+$B220$^+$ pDC population can be resolved into two subpopulations, CD4$^+$ and CD4$^-$ pDC.

negative or weakly positive for the activation markers CD40, CD80, and CD86, which are characteristics of the murine and human pDC homologue (data not shown). In brief, and as expected, no significant differences were detected in the two pDC subsets. Freshly sorted CD4$^+$ and CD4$^-$ pDCs showed similar size and homogeneous plasmacytoid morphology that was characterized by their round shape, smooth surface, and an eccentric nucleus, as shown by Giemsa staining (Fig. 2*B*). After stimulation with CpG-B, the surviving cells showed a mature DC morphology (Fig. 2*B*). These data demonstrate that both CD4$^+$ pDCs and CD4$^-$ pDCs are DC precursors and upon adaptive condition can develop into mature DCs.

To address the relationship between CD4$^+$ and CD4$^-$ pDCs, we sorted the two subpopulations of pDCs from B6 Ly5.2 mice, as shown in Fig. 2*A*. Freshly sorted CD4$^+$ or CD4$^-$ pDCs were then labeled with CFSE and injected directly intrasplenically into a separate group of sublethally irradiated (5 Gy) congenic B6 Ly5.1 mice. Three days later, the injected Ly5.2$^+$ pDCs in spleen were analyzed by flow cytometry. As shown in Fig. 2*C*, the injected CD4$^-$ pDCs demonstrated up-regulated surface CD4 expression without cell division (low CFSE cells); about half of the cells expressed medium to high levels of CD4, whereas mice injected with CD4$^+$ pDCs maintained the same or perhaps slightly increased levels of CD4 expression. It is important to note that no evidence of cell division was observed in mice that received the CD4$^-$ pDCs (Fig. 2*C*). Thus, CD4$^+$ pDCs and CD4$^-$ pDCs may represent two developing stages and at least a part of the CD4$^-$ pDCs is the immediate precursor of CD4$^+$ pDCs.

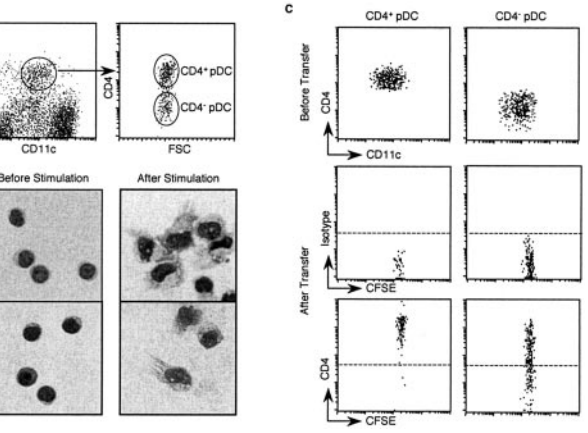

FIGURE 2. Characteristics of isolated pDC subsets. *A*, CD11c$^+$B220$^+$ pDCs were sorted into two subpopulations, CD4$^+$ and CD4$^-$, based on CD4 expression. *B*, Morphology of each pDC subset, before and after stimulation with CpG; cytospin preparations of sorted pDC subsets were stained with May-Giemsa. *C*, Adoptive transfer of pDC subsets. Freshly sorted CD4$^+$ and CD4$^-$ pDCs from B6 Ly5.2 mice were labeled with CFSE and then injected intrasplenically into B6 Ly5.1 congenic mice. Three days later, splenic cells of recipients were collected and stained with PE-CD4 or PE-isotype, PE-Cy5.5-Ly5.2, and allophycocyanin-CD11c. Donor-derived Ly5.2$^+$ cells were analyzed by four-color flow cytometry. All experiments were repeated three times with similar results.

Migration of pDC subsets after CpG stimulation in vivo

Chemokine receptors such as CCR7 are important for DC migration through the afferent lymph into the LNs (20). In humans,

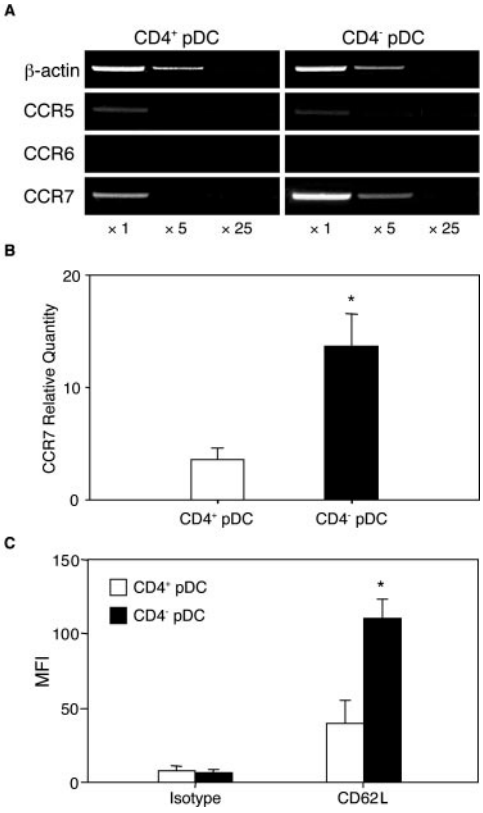

FIGURE 3. Migration-related expression in pDC subsets. *A*, Expression of CCR5, CCR6, and CCR7. Levels of mRNA transcripts and the internal control gene β-actin in the CD4$^+$ and CD4$^-$ pDCs were analyzed by RT-PCR. Primers are listed in Table I. *B*, Real-time RT-PCR determination of CCR7 expression in the CD4$^+$ and CD4$^-$ pDCs. The data shown are aggregated results of CCR7 mRNA relative quantity normalized to β-actin and presented as mean $\pm$ SD. *C*, Cellular surface CD62L expression. Isolated LD cells were stained with CD4-FITC, CD11c-PE, B220-allophycocyanin, and CD62L-biotin, followed by staining with PE-Cy5.5-conjugated streptavidin. Stained cells were analyzed by four-color flow cytometry. Mean fluorescence intensity (MFI) of CD62L included the mean $\pm$ SD of four independent experiments. CD4$^+$ pDC vs CD4$^-$ pDC; $*$, $p < 0.01$.

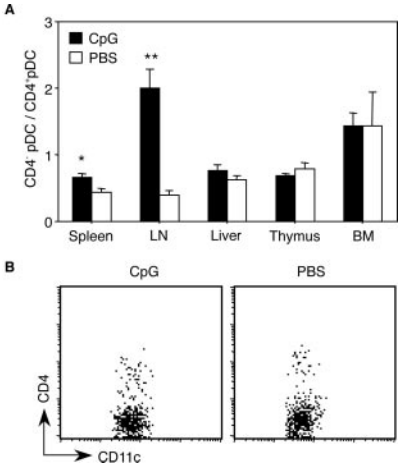

FIGURE 4. Migration of pDCs inoculated with CpG. Mice were injected i.v. with CpG-B. After 1 day, LD cells were collected from spleen, mesenteric LNs, liver, thymus, BM, and peripheral blood and stained with CD4-FITC, CD11c-PE, B220-allophycocyanin, and NK1.1-biotin, followed by staining with PE-Cy5.5-conjugated streptavidin. Percentages of $CD4^+$ and $CD4^-$ pDCs were detected by four-color flow cytometry. *A*, Ratios of $CD4^-$ cells (%):$CD4^+$ cells (%) in total pDCs were compared between CpG-B-treated and control mice. One of three independent experiments is illustrated; each group included six mice. Data represent the mean ± SD. CpG vs PBS; *, $p < 0.01$; **, $p < 0.001$. *B*, CD4 expression of peripheral blood pDCs in CpG-B and PBS-treated mice. $NK1.1^-CD11c^+B220^+$ pDCs are illustrated and data are representative of one of four experiments.

pDCs display high levels of the CCR5 and CCR7 but do not express CCR6 (21). We thus examined expression of these chemokine receptors on mouse pDCs subsets and showed that while both $CD4^+$ and $CD4^-$ pDCs expressed CCR5, the $CD4^-$ pDCs expressed almost 4-fold higher levels of CCR7 than $CD4^+$ pDCs (Fig. 3, *A* and *B*). In addition, $CD4^-$ pDCs expressed significantly higher levels of the homing marker CD62L than $CD4^+$ pDCs (Fig. 3*C*). These findings raise the question of whether $CD4^-$ pDCs are more efficient in trafficking and homing into peripheral LNs than $CD4^+$ pDCs.

To address the migration pattern of pDC subsets in vivo, we i.v. injected CpG-B into B6 mice and analyzed the frequency of $CD4^+$ and $CD4^-$ pDC subpopulations in various organs. As shown in Fig. 4*A*, CpG significantly increased proportions of $CD4^-$ pDC localized to LNs. The ratio of $CD4^-$ pDC: $CD4^+$ pDC in LNs was 3-fold increased in CpG-treated mice compared with control. Although the absolute numbers of $CD4^-$ pDCs increased ~25% in the spleen (from 2.9×10^5 to 4.1×10^5, $p < 0.05$), they increased approximately seven times in the mesenteric LNs (3.1×10^3 vs 21.6×10^3 $p < 0.001$) (Table II). In contrast, the frequency and absolute number of $CD4^+$ pDCs did not show any significant increase in either LNs or spleen. Additionally, in other tissues examined, including the BM, liver, and thymus, the proportions and

Table II. *Accumulation of pDC after CpG inoculation in vivo*[a]

	Total Cell No. ($\times 10^7$)	$CD4^+$ pDC No. ($\times 10^3$)	$CD4^-$ pDC No. ($\times 10^3$)
Spleen/CpG	13.3 ± 2.1	626.0 ± 49.5	408.3 ± 49.0*
Spleen/PBS	14.0 ± 2.6	683.0 ± 109.5	292.6 ± 22.2
LN/CpG	3.2 ± 0.9*	9.5 ± 4.7	21.6 ± 2.2**
LN/PBS	1.5 ± 0.4	7.8 ± 2.4	3.1 ± 1.3

[a] Data represent the mean ± SD. CpG vs PBS. *, $p < 0.05$, **, $p < 0.001$.

Table III. *Accumulation of pDC in inguinal nodes after local CpG inoculation*[a]

	LN Weight (mg)	Total Cell No. ($\times 10^6$)	$CD4^+$ pDC No. ($\times 10^3$)	$CD4^-$ pDC No. ($\times 10^3$)
LN/CpG	5.7 ± 1.4*	7.4 ± 1.5**	8.6 ± 3.6	16.5 ± 3.6**
LN/PBS	3.0 ± 0.5	2.2 ± 0.7	4.5 ± 1.7	3.9 ± 1.8

[a] Data represent the mean ± SD. CpG vs PBS. *, $p < 0.01$, **, $p < 0.001$.

cell numbers of both $CD4^+$ and $CD4^-$ pDCs did not show any significant change after in vivo CpG stimulation (Fig. 4*A*). Of note, no significant increase in the frequency and absolute number of $CD4^+$ pDCs appeared in the peripheral blood of CpG-treated mice (Fig. 4*B* and data not shown). These results suggest that CpG mainly drive $CD4^-$ pDC migrating from peripheral blood into the LNs.

pDCs recruit into LNs in response to infection (7, 8). To confirm the fact that indeed $CD4^-$ pDCs migrate into only inflamed LNs, we inoculated CpG-B in the left hind legs of mice to generate local inflammation and injected the same volume of PBS into the right hind leg as a control. After 1 day, bilateral inguinal nodes were excised for flow cytometric analysis. As summarized in Table III, the inguinal LN weight and total cell number in the side with CpG-B inoculation were significantly increased as compared with the controlateral (control) node. More importantly, we observed that the $CD4^-$ pDCs significantly increased in the left inguinal nodes with CpG-B inoculation. These results demonstrate that CpG is the stimulus that drives the recruitment of pDC to sentinel LNs and the predominant phenotype of these recruited pDCs is $CD4^-$ cells.

Cytokine production of pDC subsets by CpG stimulation in vitro

To examine the effect of CpG on cytokine production by pDC subsets in vitro, aliquots of freshly isolated $CD4^+$ pDCs or $CD4^-$ pDCs were cultured for 48 h with CpG-A and CpG-B, respectively. Culture supernatants were harvested and examined by ELISA for their content of secreted cytokines. As shown in Fig. 5, both the $CD4^+$ and $CD4^-$ pDCs produced higher levels of IL-6,

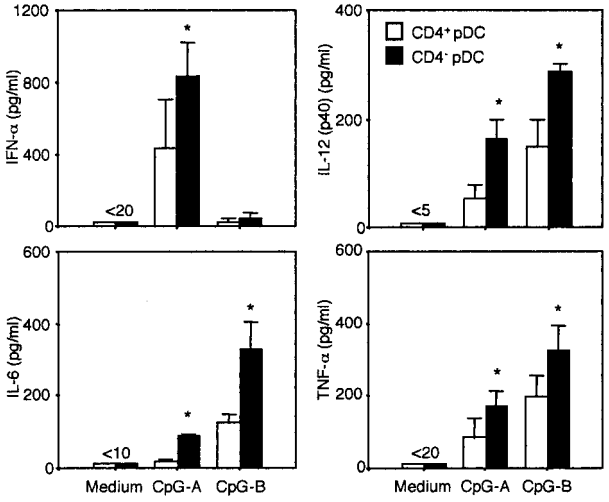

FIGURE 5. Production of cytokines in vitro stimulated with CpG. Aliquots of 3×10^4 $CD4^+$ or $CD4^-$ pDCs were cultured with CpG-A or CpG-B for 48 h. Concentrations of IFN-α, IL-6, IL-12 (p40), and TNF-α in the culture media were measured by ELISA. Data represent the mean ± SD and included three independent experiments ($CD4^+$ pDC vs $CD4^-$ pDC; *, $p < 0.05$).

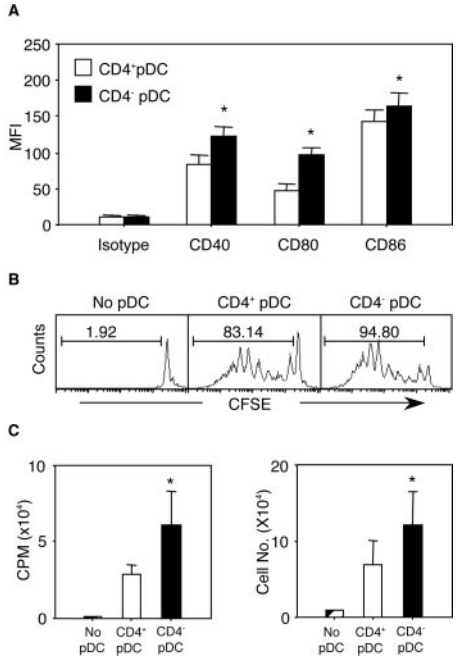

FIGURE 6. *A*, Expression of CD40, CD80, and CD86. Freshly sorted $CD4^+$ or $CD4^-$ pDCs were cultured with CpG-B. After 18-h incubation, cells were harvested and stained. MFI was analyzed by flow cytometry. *B* and *C*, T cell stimulatory capacity of pDC subsets. Freshly isolated $CD4^+$ T cells from BALB/c mice were labeled with or without CFSE and thence cultured with $CD4^+$ or $CD4^-$ pDCs in the presence or absence of CpG-B. After 5 days culture, (*B*) CFSE-labeled cells were stained with CD3-PE and CD4-biotin, followed by staining with PE-Cy5.5-conjugated streptavidin. $CD3^+CD4^+$ T cells were examined for the frequency of cell division based on CFSE dilution by flow cytometry. *C*, CFSE unlabeled cultures were pulsed with [^{3}H]thymidine for 16 h before harvesting. Cell proliferation was determined by [^{3}H]thymidine incorporation. Selected cultures were counted for viable cells. Data represent the mean ± SD and included three independent experiments ($CD4^+$ pDC vs $CD4^-$ pDC; ∗, $p < 0.05$).

IL-12 (p40), and TNF-α when stimulated with CpG-B, whereas only CpG-A induced both pDC subsets to produce IFN-α. Compared with $CD4^+$pDCs, $CD4^-$ pDCs synthesized higher selective amounts of these cytokines. It is important to note that CpG-A induced IFN-α production in $CD4^-$ pDCs at 2-fold higher than the level of $CD4^+$ pDCs. Taken together, the $CD4^-$ pDC subset in general produced significantly higher levels of cytokines than $CD4^+$ pDCs.

Allogeneic T cell activation by pDC subsets

The CpG-B studied herein has the potential to enhance the expression of costimulatory molecules expressed by the two subpopulations and stimulate them to differentiate into mature DC. However, the levels of expression of CD40, CD80, and CD86 by $CD4^-$ pDCs were significantly higher than on $CD4^+$ pDCs ($p < 0.05$) (Fig. 6*A*). To examine whether the two subsets have a different ability to activate T cells, CFSE-labeled allogeneic T cells were cultured with $CD4^+$ or $CD4^-$ pDCs in the presence or absence of CpG-B. Freshly isolated $CD4^+$ or $CD4^-$ pDC subsets without CpG addition to the cultures did not stimulate T cells to proliferate (data not shown). However, in the presence of CpG-B, both pDC subsets stimulated T cell proliferation and the stimulating capacity of $CD4^-$ pDCs was stronger than that of $CD4^+$ pDCs (95% and 83% of $CFSE^{low}$ T cells (Fig. 6*B*). These results were confirmed using the MLR assay. As seen in Fig. 6*C*, $CD4^-$ pDCs induced significantly higher T cell proliferation than $CD4^+$ pDCs. We also counted the number of viable cells after 5 days of culture and obtained similar results (Fig. 6*C*). Thus, $CD4^-$ pDCs have a greater potential to activate allogeneic T cells than $CD4^+$ pDCs.

Discussion

In this study, we have identified that following CpG stimulation, the $CD4^-$ pDCs subpopulation is the major source of pDCs that are recruited and homed to peripheral LNs. In vitro, $CD4^-$ pDC produce higher relative amounts of IFN-α, IL-12 (p40), and the proinflammatory cytokines in response to CpG. In addition, these cells also have an increased potential to activate T cell proliferation as compared with $CD4^+$ pDCs. Therefore, $CD4^-$ pDCs may provide the first line of host defense against viral infections by activating both innate and adaptive immune responses.

DCs have been shown to dictate the quality of immune response after migrating to LNs (22). Expression of CCR7 is known to drive the homing of immune cells to LNs by binding of CCR7 to the chemokines secondary lymphoid tissue chemokine or EBI1 ligand chemokine expressed on HEVs and lymphatic endothelium (23). In addition, due to CCR7 expression (21), pDC may acquire the capacity to migrate and colocalize with naive T cell and central memory T cells in the T cell areas of LNs. Of note, pDCs have been found to directly migrate from circulating blood into inflamed LNs via HEVs (3, 24). Thus, trafficking of pDCs is similar to that of naive T cells, which continually circulate from the blood to LNs via HEVs (25). In addition, CD62L interacts with L-selectin ligands expressed by HEVs (26); cell adhesion and "rolling" on HEV endothelium seem to be mediated by CD62L (27). Therefore, the higher the expression of CCR7 and CD62L by $CD4^-$ pDCs, the more these cells migrate and are recruited into LNs by CpG stimulation. Indeed, the number of pDC in LNs is decreased in L-selectin-deficient mice (9) whereas naive T cells, which express CD62L, reach the LNs through HEVs (27).

We submit that the recruitment of large numbers of $CD4^-$ pDCs into LNs is not secondary to CD4 down-regulation of $CD4^+$ pDCs. First, our transfer studies indicate that $CD4^-$ pDC acquire CD4 in recipient mice without microbial stimulation, whereas the $CD4^+$ pDC retain their level of CD4 expression (Fig. 2*C*). Similar results were observed in pDC-transferred mice that were i.v. treated with CpG (data not shown). Second, pDCs are $CD4^-$ and $CD8^-$ in the peripheral blood of normal mice (17) and animals systemically inoculated with CpG do not elicit more $CD4^+$ pDCs than controls (Fig. 4*B*). Only $CD4^-$ pDCs appear in the blood and only $CD4^-$ pDC increase in absolute numbers in LNs, providing evidence that indicate these cells represent the migrating pDCs in response to CpG stimulation. Third, the DNA-labeling kinetics suggest a developmental sequence from blood $CD4^-$ pDC to spleen $CD4^-$ pDC to spleen $CD4^+$ pDC (14). Our observations also demonstrate that $CD4^-$ pDC can immediately differentiate into $CD4^+$ pDCs without cell division. Thus, when $CD4^-$ pDCs migrate into LNs, they should differentiate into $CD4^+$ pDCs in response to inflammation. These data indicate that the increase of $CD4^+$ pDCs in LNs may be derived from the differentiation of $CD4^-$ pDCs. Previous work has suggested that pDCs that have been exposed to virus in vivo for 24 h were unable to respond to a rechallenge with the same virus in vitro to produce IFN-α (28). One explanation for this observation is that the cells had differentiated in response to virus in vivo and their more mature state was unable to produce IFN-α. In this respect, we believe that prestimulated $CD4^+$ pDCs and mature pDCs (secondary to stimulation by virus or CpG) are less responsive to CpG than $CD4^-$ pDCs.

Type I IFN plays an essential role in antiviral innate immunity. In humans and mice, pDCs are a major source of natural IFN-α-producing cells (IPCs). By stimulation of CpG-A, human pDCs

produce large amounts of IFN-α and thus are originally defined as human-specific CpG. However, CpG-A also functions on murine pDCs as we and others have demonstrated (15, 16, 29). Similarly, human type CpG-B also has a role in activating murine immune cells (30–32). Therefore, in the studies reported herein, we used CpG-A as a stimulus and report that CD4$^-$ pDCs rather than CD4$^+$ pDCs in mice are the predominant IPCs. Although the production of IFN-α by CD4$^-$ pDCs is lower than that of pDCs stimulated with virus or other CpG, we were unable to detected levels of IFN-α production by conventional CD11c$^+$B220$^-$ DCs (including myeloid CD11b$^+$ DC and lymphoid CD8$^+$ DC) stimulated with CpG-A in our culture conditions (15, 16) (data not shown). Different cell culture systems and stimuli may influence the levels of IFN-α production. In addition, low IFN-α production may due to the fact that we used a small number of pDCs (3×10^4) in our culture system. Furthermore, IFN-α induced by CpG-A, CD4$^-$ pDCs also produce large amounts of IL-12 (p40) and other proinflammatory cytokines and are more effective in inducing T cell proliferation by stimulation with CpG-B. Our in vivo adoptive transfer experiments demonstrate that CD4$^-$ pDCs are the immediate precursors of CD4$^+$ pDCs and that such development occurs without cell division (Fig. 2*C*). Therefore, when bacterial or virus infection occurs in the host, CD4$^-$ pDC precursors immediately mobilize and migrate into inflamed LNs, where they produce IFN-α and other cytokines to activate innate immunity. Upon CD4 expression, pDCs become mature and gradually lose their ability to produce cytokines following activation of T cells to initiate adaptive immune responses.

The TLRs are key molecules involved in the recognition of pathogens by the innate immune system. Signals through TLR strongly activate DC to up-regulate costimulatory molecules (CD80 and CD86) and produce proinflammatory cytokines (33, 34). The TLR9 message is restricted to pDC and is not expressed on monocyte-derived or CD11c$^+$ blood DCs, emphasizing the relationship of TLR expression to DC function (35–38). Even though there were no detectable differences of TLR9 expression between CD4$^-$ pDC and CD4$^+$ pDC subsets by semiquantitative RT-PCR (data not shown), the TLR9 ligands CpG-A and CpG-B appeared to be more effective on CD4$^-$ pDC than CD4$^+$ pDC as demonstrated by cytokine production (Fig. 5). Because there are no specific anti-mouse TLR9 Abs, it is still unclear whether there is a difference in the surface expression of TLR9 between murine spleen CD4$^+$ and CD4$^-$ pDCs.

In mice, while only CD4$^-$ pDC were found in the peripheral blood (17), both CD4$^-$ pDC and CD4$^+$ pDC have been found in the spleen, thymus, LNs, BM, and liver (9, 11, 13–16, 39). Herein, we demonstrated that the two subsets of pDCs have strikingly different immune features. In humans, however, only CD4$^+$CD11c$^-$ pDC have been found in the peripheral blood and other lymphoid tissues (40). Although the CD4$^+$CD11c$^-$ pDC have remarkable ability to secrete large amounts of IFN-α, it is not clear whether CD4$^-$ or other subsets of pDC exist in human lymph tissues as found in mice. We note that monocytes can produce IFN-α after stimulation by certain viruses, i.e., Sendai (41). Similarly, systemic lupus erythematosus (SLE) may be modulated by alterations in the functions of DC (42). In the blood of a patient with SLE, the number of CD4$^+$CD11c$^-$ CD123$^+$ pDC was reduced ~70% but serum IFN-α levels were high (42). This indicates that CD123-negative cells, which also produce IFN-α, may be elevated in SLE. In fact, large numbers of IPCs have been found in the skin of SLE patients (43, 44). This raises the possibility as to whether other pDC subpopulations such as CD4$^-$ pDC exist in tissue and whether they pathologically secrete IFN-α and migrate. We recently reported that CD4$^-$ pDCs are markedly increased in the bone marrow of NZB mice compared with control mice and that such cells produce significant amount of IFN-α (45). These data underscore the importance of CD4$^-$ pDC. Clearly, further studies of pDC distribution in vivo are required for the understanding of the mechanism of pDC immunity and the relationships between IPCs and human autoimmune diseases.

Acknowledgments

We thank Carol Oxford for FACS sorting, Loreli Coleman for mouse irradiation, and Nikki Phipps for manuscript preparation.

Disclosures

The authors have no financial conflict of interest.

References

1. Banchereau, J., and R. M. Steinman. 1998. Dendritic cells and the control of immunity. *Nature 392:245*.
2. Cella, M., F. Sallusto, and A. Lanzavecchia. 1997. Origin, maturation and antigen presenting function of dendritic cells. *Curr. Opin. Immunol. 9:10*.
3. Cella, M., D. Jarrossay, F. Facchetti, O. Alebardi, H. Nakajima, A. Lanzavecchia, and M. Colonna. 1999. Plasmacytoid monocytes migrate to inflamed lymph nodes and produce large amounts of type I interferon. *Nat. Med. 5:919*.
4. Penna, G., M. Vulcano, S. Sozzani, and L. Adorini. 2002. Differential migration behavior and chemokine production by myeloid and plasmacytoid dendritic cells. *Hum. Immunol. 63:1164*.
5. Ban, E., L. Dupre, E. Hermann, W. Rohn, C. Vendeville, B. Quatannens, P. Ricciardi-Castagnoli, A. Capron, and G. Riveau. 2000. CpG motifs induce Langerhans cell migration in vivo. *Int. Immunol. 12:737*.
6. Krepler, C., V. Wacheck, S. Strommer, G. Hartmann, P. Polterauer, K. Wolff, H. Pehamberger, and B. Jansen. 2004. CpG oligonucleotides elicit antitumor responses in a human melanoma NOD/SCID xenotransplantation model. *J. Invest. Dermatol. 122:387*.
7. Blasius, A., W. Vermi, A. Krug, F. Facchetti, M. Cella, and M. Colonna. 2004. A cell-surface molecule selectively expressed on murine natural interferon-producing cells that blocks secretion of interferon-α. *Blood 103:4201*.
8. Smith, C. M., G. T. Belz, N. S. Wilson, J. A. Villadangos, K. Shortman, F. R. Carbone, and W. R. Heath. 2003. Cutting edge: conventional CD8α^+ dendritic cells are preferentially involved in CTL priming after footpad infection with herpes simplex virus-1. *J. Immunol. 170:4437*.
9. Nakano, H., M. Yanagita, and M. D. Gunn. 2001. CD11c$^+$B220$^+$Gr-1$^+$ cells in mouse lymph nodes and spleen display characteristics of plasmacytoid dendritic cells. *J. Exp. Med. 194:1171*.
10. Bjorck, P. 2001. Isolation and characterization of plasmacytoid dendritic cells from Flt3 ligand and granulocyte-macrophage colony-stimulating factor-treated mice. *Blood 98:3520*.
11. Asselin-Paturel, C., A. Boonstra, M. Dalod, I. Durand, N. Yessaad, C. Dezutter-Dambuyant, A. Vicari, A. O'Garra, C. Biron, F. Briere, and G. Trinchieri. 2001. Mouse type I IFN-producing cells are immature APCs with plasmacytoid morphology. *Nat. Immunol. 2:1144*.
12. Ferrero, I., W. Held, A. Wilson, F. Tacchini-Cottier, F. Radtke, and H. R. MacDonald. 2002. Mouse CD11c$^+$ B220$^+$ Gr1$^+$ plasmacytoid dendritic cells develop independently of the T-cell lineage. *Blood 100:2852*.
13. Nikolic, T., G. M. Dingjan, P. J. Leenen, and R. W. Hendriks. 2002. A subfraction of B220$^+$ cells in murine bone marrow and spleen does not belong to the B cell lineage but has dendritic cell characteristics. *Eur. J. Immunol. 32:686*.
14. O'Keeffe, M., H. Hochrein, D. Vremec, I. Caminschi, J. L. Miller, E. M. Anders, L. Wu, M. H. Lahoud, S. Henri, B. Scott, et al. 2002. Mouse plasmacytoid cells: long-lived cells, heterogeneous in surface phenotype and function, that differentiate into CD8$^+$ dendritic cells only after microbial stimulus. *J. Exp. Med. 196:1307*.
15. Okada, T., Z. X. Lian, M. Naiki, A. A. Ansari, S. Ikehara, and M. E. Gershwin. 2003. Murine thymic plasmacytoid dendritic cells. *Eur. J. Immunol. 33:1012*.
16. Lian, Z. X., T. Okada, X. S. He, H. Kita, Y. J. Liu, A. A. Ansari, K. Kikuchi, S. Ikehara, and M. E. Gershwin. 2003. Heterogeneity of dendritic cells in the mouse liver: identification and characterization of four distinct populations. *J. Immunol. 170:2323*.
17. O'Keeffe, M., H. Hochrein, D. Vremec, B. Scott, P. Hertzog, L. Tatarczuch, and K. Shortman. 2003. Dendritic cell precursor populations of mouse blood: identification of the murine homologues of human blood plasmacytoid pre-DC2 and CD11c$^+$ DC1 precursors. *Blood 101:1453*.
18. Depraetere, S., L. Verhoye, G. Leclercq, and G. Leroux-Roels. 2001. Human B cell growth and differentiation in the spleen of immunodeficient mice. *J. Immunol. 166:2929*.
19. Krug, A., S. Rothenfusser, V. Hornung, B. Jahrsdorfer, S. Blackwell, Z. K. Ballas, S. Endres, A. M. Krieg, and G. Hartmann. 2001. Identification of CpG oligonucleotide sequences with high induction of IFN-α/β in plasmacytoid dendritic cells. *Eur. J. Immunol. 31:2154*.
20. Randolph, G. J. 2001. Dendritic cell migration to lymph nodes: cytokines, chemokines, and lipid mediators. *Semin. Immunol. 13:267*.
21. Penna, G., S. Sozzani, and L. Adorini. 2001. Cutting edge: selective usage of chemokine receptors by plasmacytoid dendritic cells. *J. Immunol. 167:1862*.

22. Banchereau, J., F. Briere, C. Caux, J. Davoust, S. Lebecque, Y. J. Liu, B. Pulendran, and K. Palucka. 2000. Immunobiology of dendritic cells. *Annu. Rev. Immunol. 18:767*.
23. Sallusto, F., and A. Lanzavecchia. 2000. Understanding dendritic cell and T-lymphocyte traffic through the analysis of chemokine receptor expression. *Immunol. Rev. 177:134*.
24. Yoneyama, H., K. Matsuno, Y. Zhang, T. Nishiwaki, M. Kitabatake, S. Ueha, S. Narumi, S. Morikawa, T. Ezaki, B. Lu, et al. 2004. Evidence for recruitment of plasmacytoid dendritic cell precursors to inflamed lymph nodes through high endothelial venules. *Int. Immunol. 16:915*.
25. Butcher, E. C., and L. J. Picker. 1996. Lymphocyte homing and homeostasis. *Science 272:60*.
26. Gretz, J. E., C. C. Norbury, A. O. Anderson, A. E. Proudfoot, and S. Shaw. 2000. Lymph-borne chemokines and other low molecular weight molecules reach high endothelial venules via specialized conduits while a functional barrier limits access to the lymphocyte microenvironments in lymph node cortex. *J. Exp. Med. 192:1425*.
27. Girard, J. P., and T. A. Springer. 1995. High endothelial venules (HEVs): specialized endothelium for lymphocyte migration. *Immunol. Today 16:449*.
28. Bjorck, P. 2004. Dendritic cells exposed to herpes simplex virus in vivo do not produce IFN-α after rechallenge with virus in vitro and exhibit decreased T cell alloreactivity. *J. Immunol. 172:5396*.
29. Hochrein, H., B. Schlatter, M. O'Keeffe, C. Wagner, F. Schmitz, M. Schiemann, S. Bauer, M. Suter, and H. Wagner. 2004. Herpes simplex virus type-1 induces IFN-α production via Toll-like receptor 9-dependent and -independent pathways. *Proc. Natl. Acad. Sci. USA 101:11416*.
30. Blazar, B. R., A. M. Krieg, and P. A. Taylor. 2001. Synthetic unmethylated cytosine-phosphate-guanosine oligodeoxynucleotides are potent stimulators of antileukemia responses in naive and bone marrow transplant recipients. *Blood 98:1217*.
31. Hartmann, G., R. D. Weeratna, Z. K. Ballas, P. Payette, S. Blackwell, I. Suparto, W. L. Rasmussen, M. Waldschmidt, D. Sajuthi, R. H. Purcell, et al. 2000. Delineation of a CpG phosphorothioate oligodeoxynucleotide for activating primate immune responses in vitro and in vivo. *J. Immunol. 164:1617*.
32. Weigel, B. J., N. Nath, P. A. Taylor, A. Panoskaltsis-Mortari, W. Chen, A. M. Krieg, K. Brasel, and B. R. Blazar. 2002. Comparative analysis of murine marrow-derived dendritic cells generated by Flt3L or GM-CSF/IL-4 and matured with immune stimulatory agents on the in vivo induction of antileukemia responses. *Blood 100:4169*.
33. Hertz, C. J., S. M. Kiertscher, P. J. Godowski, D. A. Bouis, M. V. Norgard, M. D. Roth, and R. L. Modlin. 2001. Microbial lipopeptides stimulate dendritic cell maturation via Toll-like receptor 2. *J. Immunol. 166:2444*.
34. Thoma-Uszynski, S., S. M. Kiertscher, M. T. Ochoa, D. A. Bouis, M. V. Norgard, K. Miyake, P. J. Godowski, M. D. Roth, and R. L. Modlin. 2000. Activation of Toll-like receptor 2 on human dendritic cells triggers induction of IL-12, but not IL-10. *J. Immunol. 165:3804*.
35. Kadowaki, N., S. Ho, S. Antonenko, R. W. Malefyt, R. A. Kastelein, F. Bazan, and Y. J. Liu. 2001. Subsets of human dendritic cell precursors express different Toll-like receptors and respond to different microbial antigens. *J. Exp. Med. 194:863*.
36. Krug, A., A. Towarowski, S. Britsch, S. Rothenfusser, V. Hornung, R. Bals, T. Giese, H. Engelmann, S. Endres, A. M. Krieg, and G. Hartmann. 2001. Toll-like receptor expression reveals CpG DNA as a unique microbial stimulus for plasmacytoid dendritic cells which synergizes with CD40 ligand to induce high amounts of IL-12. *Eur. J. Immunol. 31:3026*.
37. Hornung, V., S. Rothenfusser, S. Britsch, A. Krug, B. Jahrsdorfer, T. Giese, S. Endres, and G. Hartmann. 2002. Quantitative expression of Toll-like receptor 1–10 mRNA in cellular subsets of human peripheral blood mononuclear cells and sensitivity to CpG oligodeoxynucleotides. *J. Immunol. 168:4531*.
38. Jarrossay, D., G. Napolitani, M. Colonna, F. Sallusto, and A. Lanzavecchia. 2001. Specialization and complementarity in microbial molecule recognition by human myeloid and plasmacytoid dendritic cells. *Eur. J. Immunol. 31:3388*.
39. Dalod, M., T. P. Salazar-Mather, L. Malmgaard, C. Lewis, C. Asselin-Paturel, F. Briere, G. Trinchieri, and C. A. Biron. 2002. Interferon α/β and interleukin 12 responses to viral infections: pathways regulating dendritic cell cytokine expression in vivo. *J. Exp. Med. 195:517*.
40. Grouard, G., M. C. Rissoan, L. Filgueira, I. Durand, J. Banchereau, and Y. J. Liu. 1997. The enigmatic plasmacytoid T cells develop into dendritic cells with interleukin (IL)-3 and CD40-ligand. *J. Exp. Med. 185:1101*.
41. Fitzgerald-Bocarsly, P. 1993. Human natural interferon-α producing cells. *Pharmacol. Ther. 60:39*.
42. Palucka, A. K., J. Banchereau, P. Blanco, and V. Pascual. 2002. The interplay of dendritic cell subsets in systemic lupus erythematosus. *Immunol. Cell Biol. 80:484*.
43. Blomberg, S., M. L. Eloranta, B. Cederblad, K. Nordlin, G. V. Alm, and L. Ronnblom. 2001. Presence of cutaneous interferon-α producing cells in patients with systemic lupus erythematosus. *Lupus 10:484*.
44. Farkas, L., K. Beiske, F. Lund-Johansen, P. Brandtzaeg, and F. L. Jahnsen. 2001. Plasmacytoid dendritic cells (natural interferon-α/β-producing cells) accumulate in cutaneous lupus erythematosus lesions. *Am. J. Pathol. 159:237*.
45. Lian, Z. X., K. Kikuchi, G. X. Yang, A. A. Ansari, S. Ikehara, and M. E. Gershwin. 2004. Expansion of bone marrow IFN-α-producing dendritic cells in New Zealand Black (NZB) mice: high level expression of TLR9 and secretion of IFN-α in NZB bone marrow. *J. Immunol. 173:5283*.